

Interfiber Forces During Wetting and Drying

John Skelton

In a previous article (1) I discussed the relative importance of frictional and elastic forces in determining the mechanical behavior of textile materials, and I showed that the recovery from imposed deformation is a sensitive indicator of the magnitude of interfiber frictional force. This frictional force is determined by the normal force between fibers and by the coefficient of interfiber friction, and in the previous article these parameters were treated as constants. In fact for most polymeric materials both parameters can vary with temperature and moisture content, and during cycles of wetting and drying the frictional forces in a fibrous assembly consequently undergo a series of complex changes. The elucidation of the mechanisms of some of these changes provides an excellent example of the degree to which rather subtle physical principles are involved in a very commonplace phenomenon.

Interfiber Forces in Dry and Immersed Assemblies

As a starting point for the consideration of more complicated systems, I will discuss first the origins and nature of interfiber forces in dry and in totally immersed fibrous assemblies. Commercial textile fibers have diameters in the range of 10 to 30 micrometers (2), and at this scale the interfiber forces are mainly elastic in origin: that is, they arise because the individual fibers are in stressed configurations, and can only be maintained in these configurations through the action of forces at the points of contact with neighboring fibers. Calculations predict, and measurements confirm, that normal forces at the contact

points are typically in the range 10 to 100 micronewtons (3). This is approximately one order of magnitude greater than the Van der Waals forces between contacting cylinders of the appropriate diameter in a gaseous medium (4) and is many orders of magnitude greater than the gravitational forces in the assembly (5, 6). At normal atmospheric humidities the electrostatic forces between fibers are small, but under very dry conditions, where the resistivity of polymeric fibers is markedly increased, electrostatic forces become important (7) and can even interfere with the normal processes of textile production.

Relative motion of the components of the fibrous assembly is resisted by the frictional forces that arise as a result of the normal forces, and for bulk materials, for which the true area of intimate contact is much smaller than the geometrical area of the contacting surfaces (8), a simple proportionality exists between these two forces. However, the contact region of two crossed textile fibers, only a few square micrometers in area, is very similar to the area of true contact, and for this configuration the coefficient of friction, μ , defined as the ratio of the frictional force to the normal force, is a function of both the normal force and the diameter of the fiber (9). Since the frictional force is fundamentally a consequence of local adhesion, the magnitude of which is determined by the ratio of the shear strength to the modulus of the polymer, it is not surprising to find a strong dependence of the coefficient of fiber-fiber friction on temperature and humidity (10). As the temperature increases through the glass transition region both the shear strength and the modulus fall, though at different rates, and the ratio of

the two properties can increase or decrease: for example, the coefficient of friction for nylon falls with increasing ambient temperature between -50° and 100°C , while that of polypropylene shows a marked rise over the same temperature range. Increasing the moisture content of a polymer lowers its glass transition temperature and is equivalent in effect to a rise temperature. However, the variation of μ with humidity is a little less complex than the variation with temperature, probably because the modulus is decreased by the presence of moisture to a much greater extent than is the shear strength. Most polymers showed a marked increase in coefficient of friction with increasing humidity: an excellent illustration of this increase is found in the work of Duckett and Cheng (11), who measured the energy losses in an assembly of fibers over a wide range of atmospheric humidities.

A number of parameters controlling the interfiber frictional forces are affected when a fibrous assembly is immersed in water. Perhaps the most important change is the fall in bending modulus which occurs when most polymers are immersed in water (12). This will reduce the normal forces in open structures, but transverse swelling, which is commonly observed in textile fibers, can have the opposite effect in a densely packed assembly (13). The transverse modulus is also reduced on wetting (14), which should increase the frictional force, but the presence of liquid water at the fiber-fiber interface provides lubrication which will decrease the coefficient of friction. The net effect of these changes is usually, though not inevitably, a modest reduction in frictional force when a fibrous assembly is immersed in water. One consequence of this reduction may be readily observed: if a wad of surgical cotton is placed into water it will usually become more voluminous, partly as a direct consequence of fiber swelling, but mainly because the lowering of the frictional forces permits the fibers to move and relieve their bending stresses (15). A contrary example is provided by a tightly woven cotton canvas, which becomes dense and extremely stiff and boardy on immersion as the fibers attempt to swell against the already large restraining forces (16).

The author is an assistant director at FRL, An Albany International Company, Dedham, Massachusetts 02026.

Interfiber Forces in Drained and Drying Assemblies

If the wad of cotton discussed above is removed from the containing vessel it is immediately apparent that for fibrous assemblies the state of being wet *in* water is very different from that of being wet *with* water. As the water surrounding the wad drains away, the surface area of the water-air interface is minimized by the surface tension forces and the assembly becomes much more compact. The initial change in appearance is dramatic, but the effect on the interfiber forces is often quite small: the individual fibers are still completely surrounded by water, and the only effect of

the compressive stress caused by the diminishing interfacial area is to increase slightly the normal force between the fibers. As draining proceeds further, however, the resistance of the assembly to further contraction exceeds the driving force of the draining liquid, and air strikes through and fills the larger pores in the assembly. At this stage of drying the fibers are connected to neighboring fibers by liquid bridges at each point of contact or near contact, and the portions of the fibers not in direct contact with liquid water begin to dry.

The mechanisms and energetics of the wetting and draining of fibrous assemblies has been discussed in detail by Burgeni and

Kapur (17) and by Steiger and Kapur (18). These authors describe the refinement of an experimental technique originally used to investigate moisture equilibrium phenomena in soils (19). Their emphasis is on an understanding of the conditions leading to the maximization of the absorptive capacity of fibrous assemblies, but the data presented includes curves for hydrostatic pressure versus volume for the adsorption and exsorption processes, from which it is possible to derive the sorption hysteresis energy losses. It is interesting that these experimentally determined losses are completely consistent with the work losses calculated for the capillary deformation of a fiber mass, using literature values for the normal force per contact and the number of fiber-to-fiber contacts per unit length (20).

The magnitude of the interfiber forces set up by the liquid menisci during the late stages of drying are worthy of detailed study. The first extensive study of capillary effects between fibers was that of Preston and Nimkar (21), but some of their results were not expressed in a readily usable form. The mathematical problems associated with a complete general description of the air-water interface between contacting bodies are highly intractable (22), but for contacts between common textile fibers it is reasonable to make the assumption that the contact angle between the phases is zero and that in the final stages of drying the curvature of the meniscus is much greater than the curvature of the fiber surface. Under these circumstances the normal force between perpendicular contacting fibers is entirely attributable to the pressure differential across the air-liquid interface, and the magnitude of the force per contact is given by $2\pi DT$, where D is the fiber diameter and T is the surface tension of the liquid. The amount of liquid present in the bridge does not appear in this expression, so we may expect to find the same level of interfiber force over a wide range of moisture content. This conclusion has been verified only to a limited extent for crossed fibers, but the mathematically identical problem of the calculation of the normal force between contacting spheres, or between a sphere and a plane, has been extensively investigated, and it has been convincingly demonstrated that the normal force rapidly reaches a constant value as the amount of liquid in the capillary bridges decreases to zero (23).

The expression given above for the normal force at the contact zone is valid only for crossing fibers that are mutually perpendicular; for other crossing angles a more complicated expression is required. It is of particular interest to consider the limiting case of parallel fibers, for which

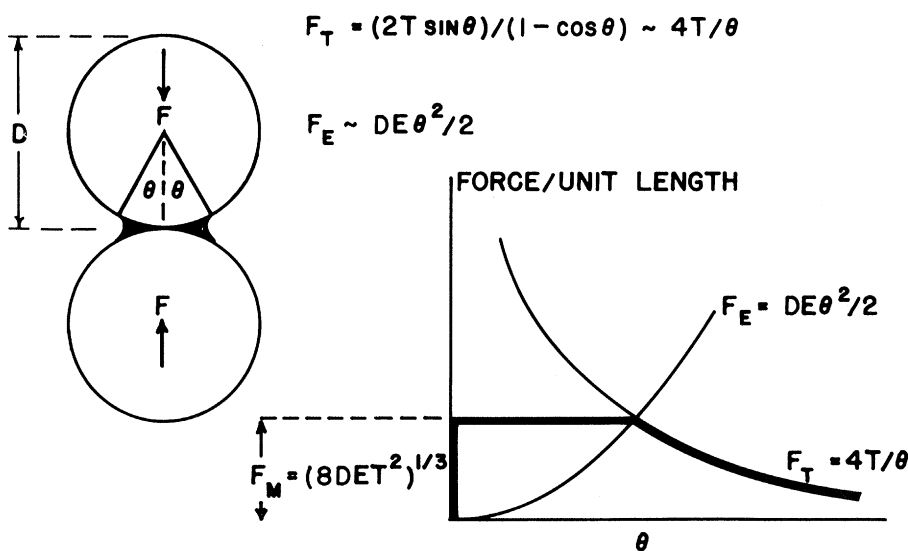


Fig. 1. Deformation of parallel contacting elastic cylinders by capillary liquid. F_T = capillary force; F_E = elastic force; and F_M = maximum interfiber force.

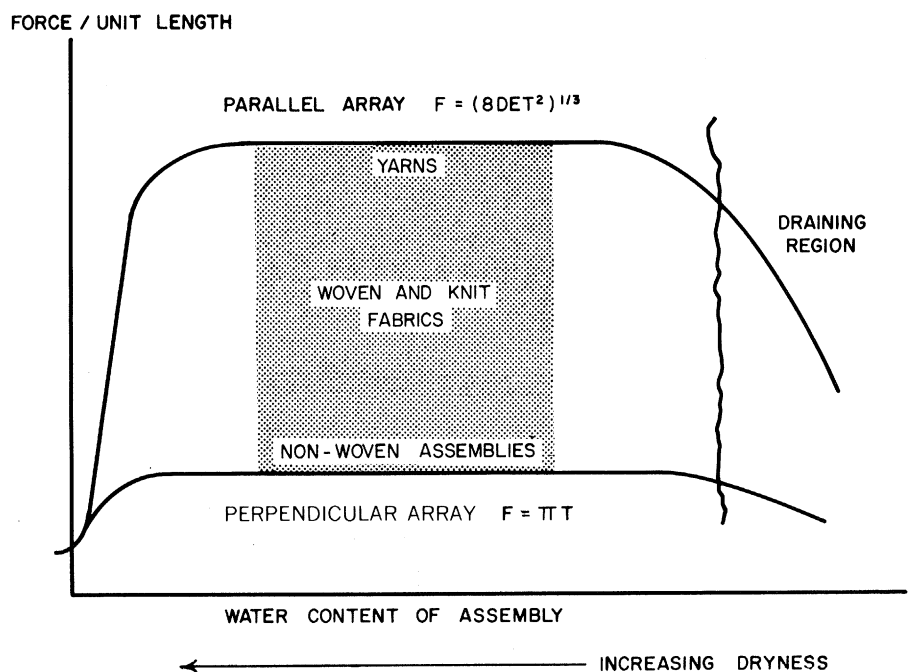


Fig. 2. Variation of normal force per unit length of fiber in various textile assemblies with changing water content.

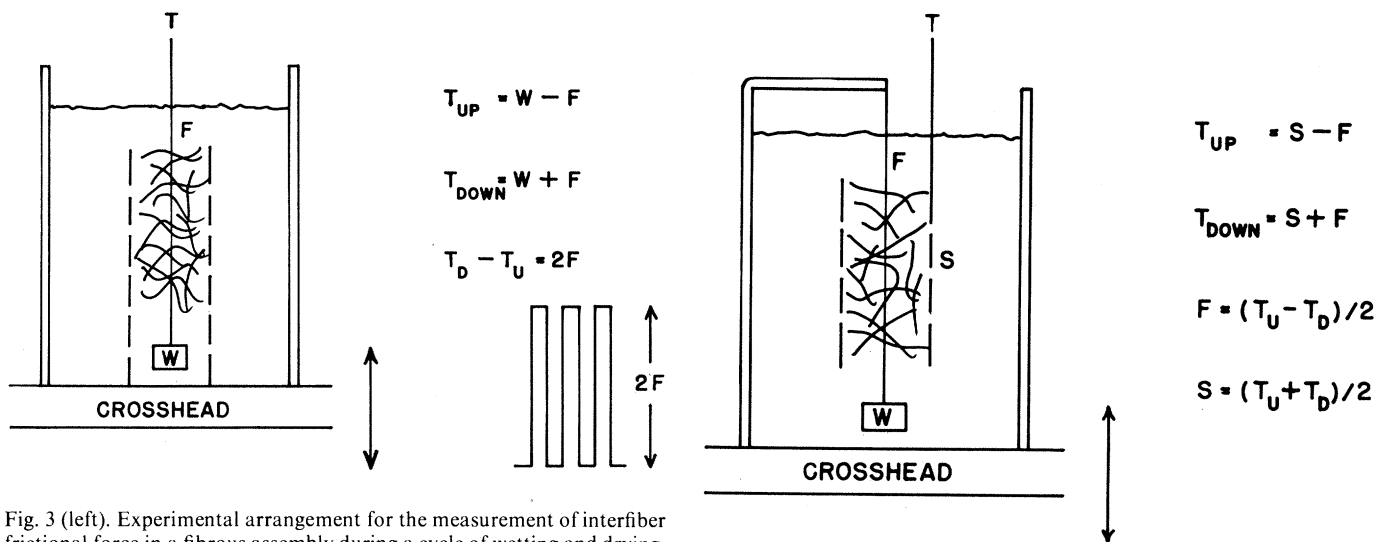


Fig. 3 (left). Experimental arrangement for the measurement of interfiber frictional force in a fibrous assembly during a cycle of wetting and drying.

T_{UP} = tension in test fiber when container is moving upward; T_{DOWN} = tension in test fiber when container is moving downward; W = tension weight; F = frictional force. Fig. 4 (right). Experimental arrangement for the simultaneous measurement of interfiber frictional force and water content of a fibrous assembly during a cycle of wetting and drying. S = weight of sample container.

the capillary force per unit length does not approach a finite limit as it does for the perpendicular crossing, but theoretically becomes infinite as the volume of capillary liquid approaches zero (22, p. 27). In actuality, the increasing normal force eventually causes local elastic deformation of the fibers, which transforms what is theoretically a line contact into an area contact, and this limits the magnitude of the force. The equilibrium between the capillary force and the elastic deformation is best explored by consideration of the half-angle θ subtended at the center of the fiber by the boundaries of the liquid bridges, defined as shown in Fig. 1. The capillary force per unit length is given approximately by $F_T = 4T/\theta$, where T is the surface tension of the liquid, while the elastic force is given by $F_E = DE\theta^2/2$, where D is the fiber diameter and E is the transverse modulus of the fiber material (24). As the volume of liquid decreases the capillary force rises according to the relationship illustrated in Fig. 1, until the elastic deformation, which tends to increase θ , is sufficient to offset the decrease in θ caused by the diminishing volume of liquid. This is a self-stabilizing configuration, and subsequent decreases in volume do not lead to an increase in the interfiber force. The maximum attainable value of the interfiber force, F_M , is given by the condition $F_M = F_E = F_T$, which implies the relationship

$$F_M = (8DET^2)^{1/3}$$

One of the interesting features of this expression is that it suggests a relatively simple technique for the determination of the transverse modulus of fine fibers, a measurement which has proved extraordinarily difficult to make (25). Preliminary measurements have been made in which

the force required to pull a fiber axially across a smooth glass plate was followed continuously as a small amount of liquid held by capillarity between the fiber and the plate was allowed to evaporate. This system is mathematically very similar (although not identical) to the system involving two parallel fibers, and the results were in good agreement with the theoretical predictions. Much work is needed to refine the experimental technique, but it shows great promise.

We have seen that the capillary force per unit length between contacting fibers reaches a limiting value for both perpendicular and parallel arrays of fibers as the amount of liquid is reduced. In fact it is possible to demonstrate that a limit is reached for all orientations of the crossing fibers, with the two cases discussed above forming the extreme values of the limit. The ratio of the two extreme values can be readily calculated. For the parallel fibers the force per unit length is given directly by the expression $F_{||} = (8DET^2)^{1/3}$. The calculation for the perpendicular crossing gives the force per contact and in order to evaluate the force per unit length of fiber we must make some assumptions con-

cerning the density of contact points. The number of contact points per unit length is inversely proportional to the diameter of the contacting fibers (6), since in physical terms the diameter of the elements of the fibrous assembly sets the scale for all the geometrical properties of the assembly. For the purpose of this discussion I have chosen a system in which the contacts are spaced apart by a distance equal to two fiber diameters, which represents an assembly with close to the maximum attainable density. For such an assembly the force per unit length of the fiber is given by $F_{\perp} = 2\pi DT \times (1/2D) = \pi T$. The ratio of the force per unit length for parallel and perpendicular assemblies is then given by

$$\begin{aligned} F_{||}/F_{\perp} &= (8DET^2)^{1/3}/\pi T \\ &\sim 0.6(DE/T)^{1/3} \end{aligned}$$

For typical textile fibers $D = 20 \mu\text{m}$, and the transverse modulus may be taken as 3.0×10^8 newton/m² (26). Substituting these values in the expression above leads to

$$F_{||}/F_{\perp} \sim 25$$

Thus the force per unit length between fibers in a parallel assembly of fibers is be-

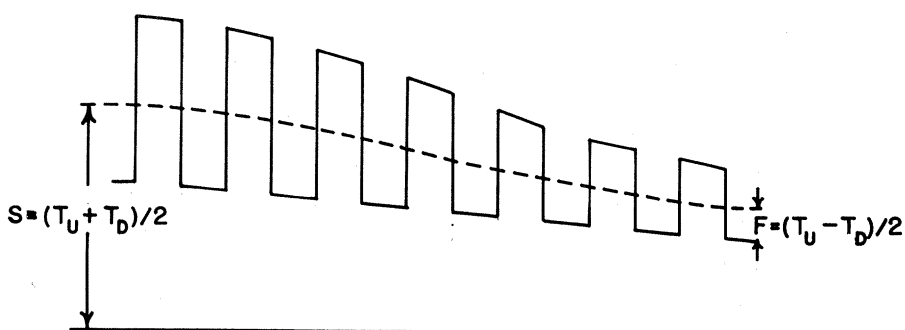


Fig. 5. Schematic experimental record for the arrangement shown in Fig. 4.

tween one and two orders of magnitude greater than the force per unit length in a perpendicular assembly. Common manifestations of the large interfiber forces in wetted parallel fibrous arrays are manifold: paint brushes rely on the phenomenon for their usefulness, and locks of wet hair are highly consolidated by the capillary forces. We are all familiar with the practice of moistening the end of a yarn before threading a needle: in this case the capillarity provides sufficient interfiber force to effectively change the yarn from an assembly of individual fibers to a monofilament, with a corresponding increase in flexural stiffness which is of the order of the number of fibers in the yarn (27)—approximately 100 for a typical yarn.

The examples mentioned above are for highly ordered parallel assemblies. In more random assemblies the number of totally parallel interfiber contact regions is much lower, and in order to estimate the average force per unit length in this case it is necessary to know the relative abundance of parallel and perpendicular contact points. This is a difficult estimate to make, but such evidence as exists suggests that the abundance of parallel contacts is approximately one order of magnitude less than the abundance of perpendicular contacts (28). Combining this information with the estimate of the relative force levels, we are led to the remarkably simple conclusion that the capillary force per unit length on a fiber will usually reach a limiting value which is to a good approximation independent of the degree of order of the

assembly, provided that it is not entirely parallel in its organization. The theoretical variation of force with moisture content for various assemblies is illustrated in Fig. 2: note that a woven fabric provides examples of both limiting types of interactions, since the fiber-to-fiber contacts within the yarns are essentially parallel in nature, while the contacts between yarns at the crossover points in the fabric are almost entirely perpendicular.

Experimental Verification

The discussion in the previous sections has been concentrated heavily on the theoretical aspects of the problems. What experimental techniques and results are available to lend support to the overall picture that has been developed of the variation of interfiber forces during wetting and drying? The simplest experimental approach involves a modification of a technique first described by Litav *et al.* (29), who used the frictional force experienced by a steel plunger passing through a wad of fibers to investigate the transmittal of compressive forces in the assembly. The substitution for the plunger of a filament identical in composition and diameter with the fibers making up the assembly permits the direct measurement of the fiber-to-fiber frictional force. Since the test filament, unlike the steel plunger, is incapable of sustaining compressive force, it is necessary to ensure that it is always under tension: a suitable experimental arrangement is

shown in Fig. 3. The fibrous assembly is constrained in an open mesh container which is continually driven up and down, and the total tension, T , is measured by a load cell and its variation with time is recorded. When the assembly is moving down the frictional force, F , adds to the tension, W , supplied by the weight, and when the assembly is moving up the frictional force is in the opposite direction. Thus the envelope of the experimental curve defines a force whose magnitude is twice the frictional force experienced by the test fiber (Fig. 3).

The entire apparatus is enclosed in a container equipped with suitable connections for filling and draining. In this way the fibrous assembly can be totally immersed and subsequently drained, and the variation of frictional force can be followed throughout a complete cycle of wetting and drying. The technique works very well, but it suffers from the shortcoming that the amount of water present in the assembly at any instant is not accurately known. Since our main interest in this investigation is the variation of frictional force with water content, it is obviously desirable to have simultaneous measurements of these two parameters. An extremely elegant modification of the original experimental arrangement, suggested by my colleague N. J. Abbott, allows these measurements to be made. The modified arrangement, which is shown in Fig. 4, differs from the previous arrangement only in that the test fiber with its tensioning weight is now driven up and down and the specimen holder and the fibrous assembly under investigation are suspended from the load cell. This duplicates all the essential features of the original arrangement, but now the frictional force is added to and subtracted from the weight, S , of the specimen and holder. A schematic experimental record is shown in Fig. 5. As before, the envelope of the curve defines the frictional force, but in addition the mean level of the curve measures the weight of the container and test assembly, and by subtracting out the known weight of the container an accurate measure of the amount of water present in the system at any instant is available.

An actual experimental record obtained using this technique is shown in Fig. 6, which illustrates many of the points mentioned earlier in the discussion. The test specimen was viscose rayon surgical wadding which had been previously wet out and dried several times in order to stabilize its response to water. In the dry state—that is, with the assembly equilibrated in air at 20°C and 65 percent relative humidity—the frictional force per unit length for

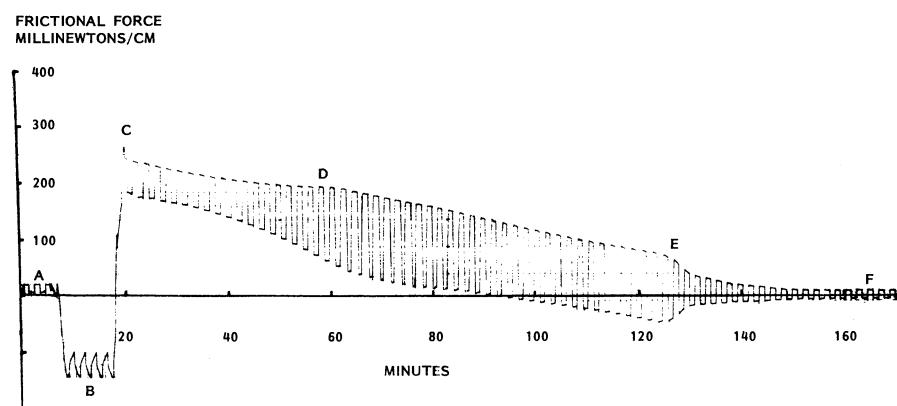


Fig. 6. Experimental record of interfiber frictional force for viscose rayon surgical wadding, showing the behavior at various stages of the wetting and drying cycle. (A) Assembly equilibrated at 65 percent relative humidity and 20°C. (B) Assembly immersed in water. Immersion reduces the average force level because of the buoyancy effect of the displaced water. As the crosshead moves up and down the specimen holder is immersed to a greater or lesser extent, and the force trace shows a sawtooth variation. (C) Assembly draining. The water content of the assembly is here a maximum, and the force trace has its highest average level. The hot air blower was started just after the removal from the water. (D) Between C and D the assembly is losing water by draining and by evaporative loss. Point D marks the initiation of capillary bridging between fibers and a marked increase in the interfiber frictional force. (E) Between D and E the assembly is losing water mainly by evaporation at an almost constant rate. The frictional force also remains constant over this range, then falls rapidly at E as the last traces of liquid water disappear. (F) The assembly is fully dry and weighs a little less than in the conditioned state at A. The hot air was switched off at F and the assembly slowly increased in weight again as moisture was absorbed from the ambient air.

the assembly was 14 millinewton/cm. On immersion this increased to 25 millinewton/cm and immediately after draining it increased again, to 59 millinewton/cm. The assembly was then fully saturated and was holding approximately 900 percent by weight of water. After a short interval the assembly was exposed to a current of hot air (60°C) which was maintained until the assembly was dry. The rapid increase in frictional force associated with the incursion of air into the assembly and the onset of the capillary mode of water retention at a water content of 700 percent is evident in Fig. 6, as is the long period of constant rate of drying during which most of the water was removed and the frictional force remained essentially constant at a value of 133 millinewton/cm, approximately ten times the force in the dry state. As the last trace of liquid water disappeared, the frictional force was rapidly and drastically reduced, and for the hot, dry assembly had the constant value 16 millinewton/cm. At this point the heater was switched off and the assembly was allowed to return to equilibrium with the original atmosphere: the small increase in weight attributable to the adsorption of water could be detected, together with a concomitant small decrease in the frictional force load to its original level. Thus, the assembly was taken through a repeatable cycle of wetting and drying, and throughout the cycle simultaneous measurements of the frictional force and water content of the assembly were made. The results were in full accord with the previous theoretical discussion.

Applications and Remaining Problems

No mention has yet been made of the usefulness of the concepts and measurements described above. This is a relatively new field of investigation, and the details of many problems have not yet been worked out. However, the ideas have considerable usefulness in many aspects of the commercial wet-finishing of textile materials. Fabrics as they are produced are often harsh and boardy to the touch, and acceptable handling characteristics are obtained only after their mechanical properties and esthetic qualities have been changed by a suitable sequence of wetting and drying operations (30). A more familiar example of this is the behavior of fabrics when they are laundered. This is a complex and difficult area of investigation and the details of the interactions are obscure, but there is no doubt that the appearance of a fabric after laundering is influenced to a large extent by the magnitude of the interfiber forces during washing and drying (31).

The concept that changes in the interfiber forces during drying can influence the mechanical properties of the dried fabric is not difficult to comprehend. However it is now becoming apparent that a deeper level of interaction exists, and recent work has suggested that the interfiber forces can affect the nature and the rate of the drying process itself (32). One area of application where an understanding of these interactions could be valuable is commercial papermaking; this consists almost entirely of a series of dewatering and drying processes, carried out at very high rates of water removal, and small increases in the drying rate can lead to large economic advantages. In fact, paper may be the ultimate manifestation of the development of interfiber forces during drying. It consists of a dense network of small cellulose fibers (33), which are brought into such intimate contact by the development of high capillary forces that hydrogen bonding is established between the fibers at the contact regions (34). In this system, therefore, the forces of interfiber bonding must increase enormously as the last traces of water are removed, and the fully dry assembly develops the high cohesion that gives paper its good mechanical strength. The development of these interfiber forces has not been studied explicitly in much detail, and this is a fascinating area for further study.

Conclusions

Many of the mechanical properties of polymeric materials are sensitive to variations in moisture content and temperature, and consequently large changes can take place in the properties of fibrous assemblies during wetting and drying. These changes are attributable to both intrinsic fiber behavior and the complex interactions between fibers in the assembly. The interactions are particularly complicated by the presence of capillary water at the contact points, and as the last traces of liquid water are removed the surface tension forces dominate the behavior of the assembly. The study of these changing interactions provides a wide variety of theoretical and experimental challenges, and leads to a new appreciation of the complexity that can underlie apparently simple processes.

References and Notes

1. J. Skelton, *Science* **177**, 657 (1972).
2. The unit used to classify synthetic textile fibers according to size is the denier. This is defined as the mass in grams of 9000 m of fiber. A comprehensive compilation of the deniers of all currently available textile fibers appears in *Modern Text.* **55**, 25 (September 1974). The denier of commercially available fiber ranges from 1 to 6, and fiber-forming polymers range in density from 0.90

g/cm³ for polypropylene to 1.54 g/cm³ for viscose rayon. These values lead to a range of fiber diameters of 10 to 30 μm [see, for example, W. H. Gloor, *Nomograms for Fiber Property Calculations* (Technical memorandum MAN64-22, Research and Technology Division, Wright-Patterson Air Force Base, Ohio, 1964)].

3. This subject is discussed briefly in (1) and in more detail in J. Skelton, *Text. Res. J.* **44**, 746 (1974).
4. F. van Vader and H. Dekker, paper presented at the Sixth International Conference on Surface Active Substances, Zurich, 1972.
5. It was shown by van Wyk (6) that the total number of fiber-to-fiber contacts per unit volume of fibrous assembly is given by $N = \pi^2 d/4$, where l is the total length of fiber of diameter d in the assembly. If we consider a unit cube filled with fibers, then the number of contacts in a layer of thickness $2d$ at the base of the assembly is $(\pi^2 d/4) \times 2d = \pi^2 d^2/2$. If the fiber has density ρ , the total weight per unit volume of the assembly is $\pi d^2 \rho/4$ and the load per contact in the bottom layer is $\rho/2l$ g or approximately $5/l$ millinewtons. If we take an upper limit of 1 g for the weight of the assembly, and assume that it is composed of 4.5-denier fibers, then from the definition of the denier (2) we can calculate that the assembly contains 2×10^5 cm of fiber. Thus, the gravitational force per contact is 2.5×10^{-2} micronewton, approximately three orders of magnitude smaller than the elastic force.
6. C. M. van Wyk, *J. Text. Inst.* **37**, T285 (1946).
7. A good overview of this subject is given in J. A. Medley, "The discharge of electrified textiles," *ibid.* **45**, T123 (1954). At low humidities the resistivity of most textile materials is sufficiently great that charges persist on the fibers for long times. The greatest charge density that can be sustained in dry air on a fiber of textile dimensions is approximately 2×10^{-8} coulomb/cm², equivalent to an axial line charge density, λ , of approximately 1×10^{-10} coulomb/cm. The maximum mutual force between two such charged fibers at a perpendicular contact point is approximately given by $\lambda^2/\pi = 3 \times 10^{-1}$ micronewton per contact. This is small compared to the elastic force, but it is one order of magnitude greater than the gravitational force. The electrostatic force between fibers is usually repulsive, and the calculation presented above makes it clear that it will be sufficient to cause disruption of a fibrous assembly in the absence of any greater cohesive forces. In many textile forming processes, where fibers are being manipulated into the orderly arrays characteristic of finished textile products, the cohesive forces are low, and control of static electrification becomes of major concern.
8. An excellent review of measurement techniques available for estimating the true size of contact areas in bulk materials is given in E. Rabinowicz, *Friction and Wear of Materials* (Wiley, New York, 1965), chap. 3. The quoted values of junction diameter range from 5 to 31 μm, with most of the values lying between 5 and 10 μm.
9. F. P. Bowden and D. Tabor, *The Friction and Lubrication of Solids* (Oxford Univ. Press, London, 1964), part 2, chap. 8.
10. J. K. Lancaster, *Plast. Polym.* **41**, 297 (1973).
11. K. E. Duckett and C. C. Cheng, *Text. Res. J.* **44**, 365 (1974).
12. H. M. Elder, *J. Text. Inst.* **57**, T75 (1966).
13. N. J. Abbott, F. Khoury, L. Barish, *ibid.* **55**, T111 (1964).
14. S. Morris, *ibid.* **59**, 536 (1968).
15. Steiger and Kapur (18) observed experimentally that random fiber assemblies with densities greater than 0.2 g/cm³ increase in volume on wetting, while less dense assemblies usually decrease in volume. It is possible to demonstrate that this behavior is in full accord with the ratio of the elastic and surface tensional forces in assemblies of various densities.
16. F. T. Peirce, *J. Text. Inst.* **28**, T45 (1937).
17. A. A. Burgeni and C. Kapur, *Text. Res. J.* **37**, 356 (1967).
18. F. M. Steiger and C. Kapur, *ibid.* **42**, 443 (1972).
19. The technique was first described by W. B. Haines, *J. Agric. Sci.* **20**, 97 (1930). This is the final paper of a series [*ibid.* **15**, 529 (1925); R. A. Fisher, *ibid.* **16**, 492 (1926); W. B. Haines, *ibid.* **17**, 264 (1927); R. A. Fisher, *ibid.* **18**, 406 (1928)] in which Haines and Fisher first explored, with a great deal of mutual hostility, the nature of capillarity in multicomponent assemblies, and established the important concept of capillary hysteresis.
20. J. Skelton, *Text. Res. J.* **45**, 540 (1975).
21. J. M. Preston and M. V. Nimkar, *J. Text. Inst.* **43**, T402 (1952).
22. For an excellent review of this subject see H. M. Princen, in *Surface and Colloid Science*, E. Matijevic, Ed. (Wiley-Interscience, New York, 1969), vol. 2, chap. 1.
23. N. L. Cross and R. G. Picknett, in *Proceedings of International Conference on Mechanism of Corro-*

- sion of Fuel Impurities, Marchwood, England (1963), p. 383; G. Mason and W. C. Clark, *Chem. Eng. Sci.* **20**, 854 (1965); T. Gillespie and G. D. Rose, *J. Colloid Interface Sci.* **24**, 246 (1967).
24. The exact expression for the capillary force per unit length between two contacting parallel cylinders is $F_T = 2T \sin \theta / (1 - \cos \theta)$, which for small values of θ can be reduced to $F_T = 4T / \theta$. The relationship between the deforming force per unit length, F_E , and the elastic deformation of two contacting parallel cylinders is given, for example, in R. J. Roark, *Formulas for Stress and Strain* (McGraw-Hill, New York, ed. 4, 1965), chap. 13, table XIV. It may be written $b = 2.15(PD/2E)^{1/2}$ for identical cylinders of diameter D and Poisson's ratio 0.3, where b is the width of the contact zone. The angle θ may be written as $\theta = b/D$, which leads to $F_E = DE\theta^2/2$ approximately, as in the text.
 25. S. L. Phoenix and J. Skelton [*Text. Res. J.* **44**, 934 (1974)] summarize the available data and present new measurements for fibers of textile dimensions.
 26. Values of 2.4×10^8 and 4.0×10^8 newton/m² were found by Phoenix and Skelton (25) for polyester and nylon fibers, respectively. A value of 3.0×10^8 newton/m² is reasonable for the approximate calculations presented here.
 27. The flexural rigidity of a filament is proportional to d^4 , where d is the diameter of the filament. Thus a yarn composed of n independent filaments has a total flexural rigidity proportional to nd^4 . If the filaments are consolidated, the yarn behaves as a cylinder of diameter D , where $D^2 \sim nd^2$. Thus the ratio, k , of the yarn stiffness with and without consolidation is $k \sim D^4/nd^4 = n^2d^2/nd^4 = n$.
 28. A. E. Stearn, *J. Text. Inst.* **62**, T353 (1971).
 29. Y. Litav *et al.*, *ibid.* **63**, T 224 (1972).
 30. Typical examples of the magnitudes of the changes in fabric bending behavior brought about by finishing treatments are given in J. D. Owen, *ibid.* **59**, T313 (1968).
 31. V. Köpke and H. A. Nordby, *ibid.* **71**, T458 (1970); E. Nielsen and H. M. Elder, *ibid.* **65**, T488 (1974).
 32. M. S. Nassar, M. Chaikin, A. Datyner, *ibid.* **65**, T464 (1974); *ibid.* **64**, T718 (1973).
 33. The fibers in paper made from wood pulp commonly take the form of flattened ribbons. These ribbons are typically 20 to 40 μ m long, 30 to 40 μ m wide, and a few micrometers thick. Paper differs from the textile assemblies that we have been considering in that the flattened cross section permits the establishment of large areas of molecularly close contact on drying.
 34. See, for example, A. M. Nissan, in *The Formation and Structure of Paper*, F. Bolam, Ed. (British Paper and Board Makers Association, London, 1962), p. 119.

Lymphocyte Surface Immunoglobulins

Molecular properties and function as receptors for antigen are discussed.

John J. Marchalonis

Recognition of nonself antigenic configurations on infectious agents, tumors, and assorted macromolecules is mediated by specific receptors that occur on the surface of lymphocytes. Knowledge of the nature of these recognition molecules is critical to an understanding of the mechanisms of immune function. Although immunologists have pondered the problem of antigen recognition for over 70 years (1), studies that provide definite information on the molecular properties of lymphocyte receptors for antigen were performed only within the past few years. It is now possible to draw general conclusions regarding antigen-specific receptors on bone marrow-derived lymphocytes (B cells) and on thymus-derived lymphocytes (T cells). The viewpoint I develop in this article is that membrane-associated immunoglobulin related to the immune macroglobulin antibodies (that is, the immunoglobulin M, or IgM, class) serves a recognition role in many immunologically specific reactions of both B and T lymphocytes.

Basic properties of lymphocyte populations. Members of lymphocyte populations within an individual animal are phenotypically restricted in their capacity

to respond to antigens. In accordance with the clonal selection hypothesis of Burnet (2), sometime during the ontogenetic development of lymphocytes, the individual cells become committed to the extent that each lymphocyte can respond to only one antigen. It is thought that each cell expresses on its surface one type of receptor for antigen. Combination of the proper antigen with this receptor initiates the chain of immune differentiation that results in the production of antibodies to the antigen. The most obvious molecular candidate for the role of cell surface receptor for antigen is the antibody itself; a conjecture that was stated as early as 1900 by Ehrlich (1). However, direct proof of this "minimal hypothesis" has been difficult to attain for two reasons. First, clonal restriction of the response made precise studies arduous because few cells in a normal population—for example, usually at most only one cell in a thousand (3)—respond to a given antigen. This problem necessitated the development of methods capable of analyzing binding of antigen by individual cells and hindered quantitative biochemical approaches that measure bulk or average properties of a cell population. The second problem arises from recent discoveries that functionally distinct classes of lymphocytes exist and play specialized roles in the generation of an immune response.

Lymphocytes in the mouse and in various other mammals and birds can be divided into two broad categories on the basis of surface markers and functional properties (4). Such cells develop in ontogeny from cells of the hemopoietic system. Hemopoietic stem cells arise in the yolk sac of the embryo and localize in the bone marrow of the adult mammal. The stem cells ancestral to lymphocytes are generated in the bone marrow, but migrate to primary lymphoid organs such as the thymus and the bursa of Fabricius in birds or the bursal equivalent in mammals where they differentiate, respectively, into T cells and B cells. Both types of cells possess specific receptors for antigen. The B cells are the precursors of antibody-forming cells, whereas T cells are responsible for cell-mediated immune reactions such as rejection of allografts, elimination of tumors, and delayed hypersensitivity reactions and, moreover, can act as "helper cells" that collaborate with B cells in the generation of antibodies to certain antigens. Largely because of the ease with which surface immunoglobulin is demonstrable on B cells, the present consensus is that the receptor for antigen on these cells must be immunoglobulin. The situation has not been so clear with T lymphocytes. In the first place, it has been considerably more difficult to detect surface immunoglobulin on T cells than on B cells, and varied results have been reported. As is cited below, surface immunoglobulin of T cells has now been shown by a number of techniques. Another aspect of the problem clouding the nature of the T lymphocyte receptor for antigen stems from the fact that all functions carried out by T lymphocytes are not necessarily immunological (5, 6), and it is inaccurate to speak of "the" T cell receptor. In general, it might be more apt to restrict comments to T cells carrying out a particular function.

Some of the heterogeneity of surface recognition processes of lymphocytes are shown in Fig. 1, by presenting a hypothetical scheme depicting the evolutionary ori-

The author is head of the Molecular Immunology Laboratory, The Walter and Eliza Hall Institute of Medical Research, P.O., Royal Melbourne Hospital, Victoria 3050, Australia.